Hydrogeology Journal (2022) 30:401–415
https://doi.org/10.1007/s10040-022-02460-1

REPORT

Seasonal variations and long-term trends of groundwater over the Canadian landmass

Junhua Li[1] · Shusen Wang[1]

Received: 12 March 2021 / Accepted: 22 January 2022 / Published online: 15 February 2022

Abstract

Detailed knowledge of groundwater storage improves the understanding and management of water resources. Observations from Gravity Recovery and Climate Experiment (GRACE) satellites have provided data on global terrestrial-water-storage (TWS) changes since 2002. Combining GRACE-TWS and land-surface model (LSM) estimates of soil water, snow-water equivalent and surface-water storage provides a method to quantify groundwater storage (W_{ground}). This study examines the W_{ground} seasonal variations and trends for Canada's landmass during the period 2003–2016 using GRACE-TWS and the Canadian LSM EALCO (Ecological Assimilation of Land and Climate Observations) model. The results show the study region has a maximum seasonal variation (ΔW_{ground}) of 118 mm (volume equivalent 700 km^3), with the maximum/minimum W_{ground} appearing in July/April. Eastern Canada has relatively large ΔW_{ground} values, up to 400 mm in Newfoundland. The Prairie region has the smallest value (<50 mm). The western and central regions show the maximum/minimum W_{ground} mostly in spring/fall. In contrast, eastern Canada has the maximum/minimum W_{ground} mostly in fall/spring. South Ontario and the Prairie area show the maximum/minimum W_{ground} in summer/winter. Additionally, the W_{ground} trends over the 14-year study period present large spatial variability, with increasing trends of up to 10 mm/year in eastern Canada and decreasing trends (similar magnitudes) in the west. The increasing trend largely offsets the decreasing trend in the study area, and the overall W_{ground} for the region does not show a significant trend during 2003–2016. Comparison of W_{ground} with groundwater well measurements present similar long-term trends but with a phase difference in seasonal variations.

Keywords Groundwater · Remote and satellite sensing · Climate change · EALCO model · Cold regions hydrogeology

Introduction

Groundwater, as the largest freshwater storage component of the hydrological systems, is an essential resource necessary to sustain agricultural, industrial, and domestic activities in Canada. About one third of Canadians depends on groundwater for drinking water and up to 80% of Canada's rural population uses groundwater for its entire water supply (Council of Canadian Academies 2009). Groundwater also plays an important role in sustaining ecosystems and the water cycle's response to climate change at regional and global scales. Increased human withdrawals of groundwater or changes in climate have resulted in growing pressure on groundwater resources, which poses a serious threat to water security and potentially causes a decline in agricultural productivity and energy production (Frappart and Ramillien 2018). Monitoring and understanding groundwater storage changes is thus critical for maintaining sustainable economic development and healthy ecosystems, and for better understanding the hydrological cycles and climate change (Chen et al. 2016).

Monitoring and quantifying groundwater is difficult because it deals with water in a complex subsurface environment. Well monitoring is the traditional approach for estimating groundwater storage but often needs knowledge of the aquifer structure and some critical parameters such as transmissivity and storativity (or specific yield), which are difficult to obtain. In addition, well monitoring is not spatially continuous and has a high cost for a large region. There are very limited wells in some areas, especially in remote and harsh environments such as cold regions in Canada due to difficulties of access and monitoring.

✉ Shusen Wang
Shusen.Wang@canada.ca

Junhua Li
Junhua.Li@canada.ca

[1] Canada Centre for Remote Sensing, Natural Resources Canada, Ottawa, Ontario K2A 0E4, Canada

Satellite remote sensing is increasingly being used in hydrological studies for its large spatial coverage and cost-effectiveness, and its ability to provide data in a timely manner. The Gravity Recovery and Climate Experiment (GRACE) satellite mission, launched in 2002, provides a unique approach to detect gravity changes globally due to redistribution of mass in the Earth system (Tapley et al. 2004). By separating the contributions to mass changes, GRACE-observed gravity changes can be used to derive terrestrial water storage (TWS) change, which includes the changes of groundwater storage (W_{ground}), soil-water content (W_{soil}), snow-water equivalent (W_{snow}), and surface-water storage (W_{surf}). Thus, GRACE provides a practical way to estimate W_{ground} when W_{soil}, W_{snow} and W_{surf} can be estimated.

The GRACE TWS data have been used to quantify variations and long-term trends of W_{ground} at regional and global scales in various studies (e.g., Rodell et al. 2007, 2009; Swenson et al. 2006; Famiglietti et al. 2011; Richey 2014; Huang et al. 2016; Bahanja et al. 2018; Shamsudduha and Taylor 2020; Opie et al. 2020). As GRACE cannot separate the different components of TWS, the W_{soil}, W_{snow} and W_{surf} estimated from other independent approaches such as land-surface models (LSMs), were usually used to separate W_{ground} from GRACE TWS. Famiglietti et al. (2011) and Scanlon et al. (2012) analyzed long-term W_{ground} change in the California Central Valley (USA) region by combining TWS from GRACE, W_{soil} from GLDAS (Global Land Data Assimilation System) LSMs, W_{snow} from the Snow Data Assimilation System (SNODAS) datasets, and W_{surf} from in-situ surface-water reservoir measurements. Thomas and Famiglietti (2019) extended the analysis of groundwater change in USA by using W_{soil} and W_{surf} (surrogated by surface runoff) from GLDAS LSMs, W_{snow} from SNODAS, and GRACE TWS, and identified climate-induced groundwater depletion.

While the GRACE satellite mission provides an innovative tool for groundwater estimation through its integration with other independent in-situ and model data sources, so far studies and information on the groundwater climatology for Canada's landmass are still very limited. On the other hand, the vast majority of the existing studies, as mentioned before, have relied on the land-surface models (LSMs) included in GLDAS. Applying uncalibrated and unvalidated global-scale models to a region involves high uncertainty. This is particularly so for Canada where the hydrological processes are much more complex due to the cold-region processes dominating the landmass such as snow accumulation/melt and soil freeze/thaw. Indeed, model comparison studies have revealed large biases and uncertainties in simulating the water cycle over Canada's landmass (Wang et al. 2015a; Xia et al. 2015; Mortimer et al. 2020). EALCO (Ecological Assimilation of Land and Climate Observations model) has been developed by Natural Resources Canada with a specific focus on cold-region mechanisms for land-surface radiation transfer, energy balance, water dynamics, and carbon and nitrogen biogeochemical cycles which play various roles in the physiological and ecohydrological processes. In particular, the freeze/thaw processes for soils, lakes and snow cover, and the remote-sensing-based vegetation and land-surface dynamics (e.g., albedo, surface-water cover), have demonstrated robustness in a number of international LSM intercomparison studies (Zhang et al. 2008; Widlowski et al. 2011; Wang et al. 2014, 2015a, b). This gave confidence in using EALCO results for this study on the Canadian landmass.

While EALCO includes lake/river surface evaporation simulations, it does not include the river routing process so it is difficult to apply its results (e.g., snowmelt) directly in this study. In many published studies, surface water is ignored (Huang et al. 2016; Chen et al. 2014; Rodell et al. 2007), while in some others LSM-simulated surface runoff is used as a proxy for surface-water storage change (Shamsudduha and Taylor 2020; Thomas and Famiglietti 2019). In this study, EALCO-simulated surface runoff is used as a proxy for surface-water storage.

The objective of this study is to assess the seasonal variations and long-term trends of the W_{ground} for Canada's landmass for the period 2003–2016 using the TWS from GRACE monthly spherical harmonic (SH) solutions and the W_{soil}, W_{snow} and W_{surf} values from the Canadian LSM of EALCO. This study calculates a suite of parameters representing the spatial and temporal variations of W_{ground}, including the occurrence time and the interannual variability of the maximum and minimum W_{ground} in a year, the range of seasonal variation of W_{ground} and its interannual variability, and the long-term trend of W_{ground} over 2003–2016. The results are presented in national maps and aggregated into the hydrological units of the major drainage areas (MDAs) of Canada. The GRACE SH-derived W_{ground} is also compared to those derived from two GRACE monthly Mascon solutions and the groundwater well measurements.

Data and methods

TWS variations in most cases are mainly contributed by the changes in W_{ground}, W_{snow}, and W_{surf}. In this study, W_{ground} is computed as

$$W_{ground} = \mathrm{TWS} - W_{soil} - W_{snow} - W_{surf} \quad (1)$$

The TWS used in this study includes the GRACE monthly SH solutions (Landerer 2020), containing monthly TWS changes processed by three different data processing centers: the Center for Space Research (CSR; University of Texas, USA), GeoForschungsZentrum (GFZ; Potsdam, Germany),

and Jet Propulsion Laboratory (JPL, USA). The TWS data were downloaded from the GRACE Tellus website (JPL 2020). All three TWS datasets were processed from the latest release RL-06 V03 with 1° × 1° global grids. The datasets were calibrated with standard corrections including a glacial isostatic adjustment (GIA). Post-processing filters including a de-stripping filter and a 300-km-wide Gaussian smoothing filter were applied to reduce correlated errors (Landerer and Swenson 2012). Scaling coefficients for the global land grids were applied to restore much of the energy removed by the postprocessing filtering. A detailed description of the data processing is available in Landerer and Swenson (2012). The monthly TWS data are anomalies to the baseline average over the study period of January 2003 to December 2016. Note that the baseline in the original datasets is the average over the period of January 2004 to December 2009. Because the differences among the three TWS datasets were found to be small over the study region (Wang and Li 2016), the averages of the three datasets were used in this analysis. For the result comparisons, two other TWS products derived from the GRACE monthly Mascon solutions (GRCTellus. JPL RL06M.MSCNv02 and CSR RL06M.MSCNv02) were also used in this study. More detail about the Mascon solution data can be found in Wiese et al. (2018). There are 13 months with missing GRACE TWS data during the study period, which include June 2003, January and June 2011, May 2012, March and September 2013, February 2014, May, October and November 2015, and April, September and October 2016.

To estimate GRACE-derived W_{ground} in Eq. (1), the simulated soil moisture W_{soil}, snow water equivalent W_{snow}, and surface runoff (as a proxy for surface-water storage W_{surf}) from the LSM EALCO were used. EALCO is driven by climate forcing at a half-hourly time step and 5-km spatial resolution. The monthly W_{soil} data include water contained in the soil column of up to 4.0 m depth including seven soil layers (0–10, 10–20, 20–40, 40–80, 80–140, 140–240, 240–400 cm). When the water table is above the bottom of the seventh layer (i.e., 4.0 m), the soil layers below the water table will be exposed to groundwater and the actual number of soil (unsaturated) layers will be determined by the actual depth of the water table. The monthly W_{soil}, W_{snow} and W_{surf} for the period 2003–2016 are calculated from the half-hourly EALCO W_{soil}, W_{snow} and W_{surf} values based on the actual days used for each GRACE monthly solution. Since the GRACE TWS data are anomalies relative to the baseline average over the study period, the W_{soil}, W_{snow} and W_{surf} anomalies were calculated by subtracting the time-mean baseline over the same period to make EALCO and GRACE data comparable.

Eight parameters are calculated from the derived monthly W_{ground} data to characterize the spatiotemporal variations of W_{ground} (Table 1). They include: the long-term trend (τ) represented by the Thiel-Sen linear regression slope of monthly W_{ground} time series for 2003–2016; the months with maximum/minimum W_{ground} in a year (M_{max}/M_{min}) and their interannual variations ($\sigma_{max}/\sigma_{min}$); and the range of seasonal W_{ground} variation (ΔW_{ground}) and its interannual variations (represented by the standard deviation $\sigma_{\Delta ground}$ and the coefficient of variance COV of ΔW_{ground}). For the calculation of σ_{max} and σ_{min}, if the difference of M_{max} (or M_{min}) among different years is larger than 6, the difference is subtracted by 12.

The study area is shown in Fig. 1. It covers most of the Canadian landmass except areas (the grey area in Fig. 1) having no groundwater recharge due to permafrost as simulated by the EALCO model—Fig. S1 of the electronic supplementary material (ESM)—or snow/ice covering probability larger than 50% in the warm season (Fig. S2 of the ESM, Trishchenko and Ungureanu 2021). The study region includes eight MDAs of Canada. The GRACE TWS data are provided in 1° × 1° grids, but the actual resolution is much coarser (>350 km × 350 km). The Rocky Mountains with permanent snow/ice occupies a large portion of the Pacific MDA and the remaining regions (e.g., west coast) barely fits this coarse resolution. The GRACE grid often includes fractional areas of permanent snow/ice; therefore, the entire Pacific MDA is excluded in the analysis. The study also excludes the Mississippi River MDA due to its small area (~27,000 km^2). All the results are presented in national maps under the Lambert Conformal Conic (LCC) projection and are also aggregated into the MDAs. The MDAs provide hydrological units that are frequently used for data collection and compilation, and for spatial analysis of environmental, economic and social statistics (Statistics Canada 2003).

Daily groundwater level data from groundwater observation wells available in two GRACE grids in the Nelson River MDA and the St. Lawrence MDA are used for W_{ground} comparisons. The well data for groundwater level (W_{level}) can be downloaded from the Groundwater Information Network (GIN) portal (GIN 2021), which connects Alberta's groundwater observation well network (GOWN), and the Quebec groundwater monitoring network (QGMN 2021). For the study period, there are multiple wells with either partial or complete data for both comparison grids. For each grid, the wells that have a long overlap monitoring period with the study period are selected. These include four wells located in the Nelson River MDA and six wells in the St. Lawrence MDA (Fig. 1). Monthly well data are obtained by averaging the daily data for each month, and subtracting their respective time-mean baseline. It was noted that the wells in the Nelson River MDA and the St. Lawrence MDA have observations covering the time periods of 2003–2016 and 2005–2016, separately. Finally, the mean W_{level} change of the wells in each comparison grid is calculated to represent the W_{level} change for that specific grid.

Table 1 Parameters used for characterizing W_{ground}

Variable	Unit	Description
M_{max}	–	The month with maximum W_{ground} in a year
M_{min}	–	The month with minimum W_{ground} in a year
σ_{max}	Month	Interannual variation of M_{max} (1 standard deviation, SD) over 2003–2016
σ_{min}	Month	Interannual variation of M_{min} (1 SD) over 2003–2016
ΔW_{ground}	mm	Range of seasonal variation of W_{ground}, averaged over 2003–2016
$\sigma_{\Delta Wground}$	mm	Interannual variation of ΔW_{ground} (1 SD) over 2003–2016
COV	–	Coefficient of variance of ΔW_{ground} ($\sigma_{\Delta Wground}$ /ΔW_{ground}) over 2003–2016
τ	mm/year	Trend (Thiel-Sen regression slope) of W_{ground} over 2003–2016

Results

Seasonal variations of W_{ground}

Figure 2 shows the average monthly W_{ground} over 2003–2016 and provides a general overview of the spatial and seasonal variations of W_{ground} over the study area. In January, W_{ground} presents small spatial variation across the study area with a value around the annual average (0 mm) over the study period. From February to June, the W_{ground} in the western region (including the Western and Northern Hudson Bay, the Great Slave Lake, and the Arctic MDAs) and the Southern Hudson Bay area slightly increases till early spring, after which the W_{ground} rapidly increases and reaches its yearly highest value in June due to high groundwater recharge after snowmelt and soil thaw. For example, the Southern Hudson Bay MDA has the highest W_{ground} (~75 mm above the annual average) in June and the Western and Northern Hudson Bay MDA has the highest W_{ground} (~ 50 mm above the annual average) in June. In contrast, the W_{ground} in east Canada gradually decreases during this period and mostly reaches its lowest value until snowmelt and soil thaw start. South Canada, from southern Ontario to east Prairie and including the Maritime Provinces, reaches the lowest W_{ground} in March or April—for example, the Maritime Provinces MDA and the south portion of the St. Lawrence MDA (mainly in south Ontario), reaches the lowest W_{ground} of ~100 mm below the annual average in April. After that, the W_{ground} rapidly increases

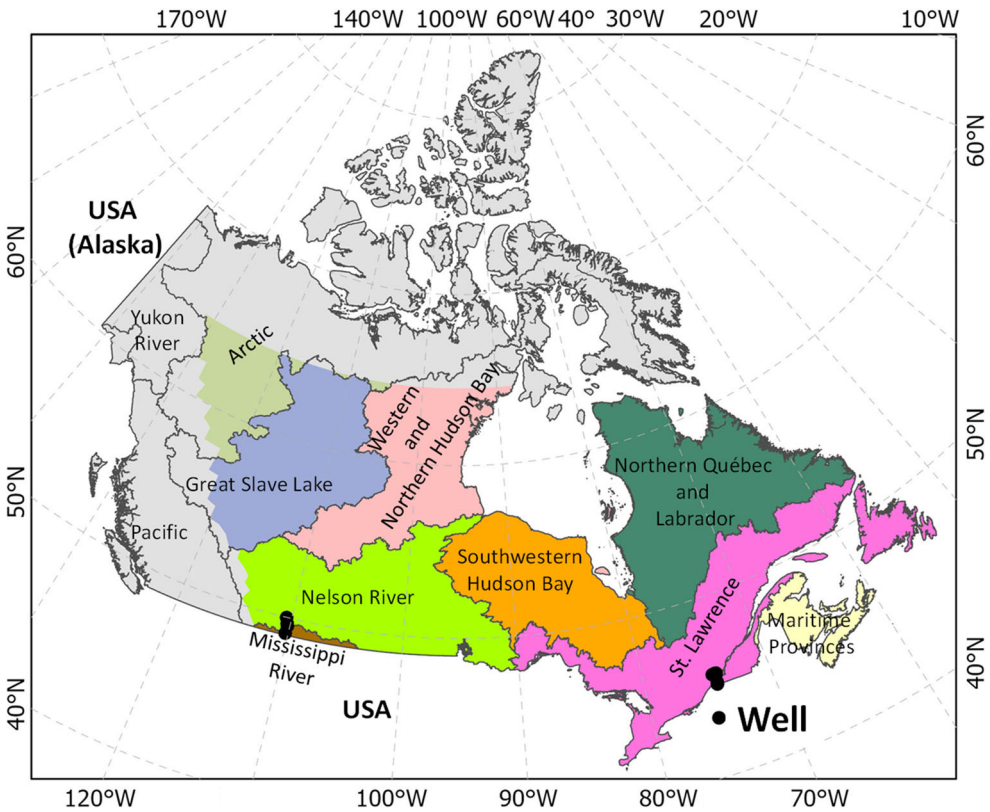

Fig. 1 Map of the study region, covering eight major drainage areas (MDAs, polygons shown in colors) over Canada's landmass. Note that the Nelson River MDA excluded a small portion in the west, the Western and Northern Hudson Bay MDA excluded the portion in high Arctic, the Great Slave Lake MDA excluded a small portion in the north and the west, and the Arctic MDA only included its southern part. The grey areas, having permafrost or permanent snow/glacier probability larger than 50%, or areas smaller than the GRACE footprint, are excluded in this study

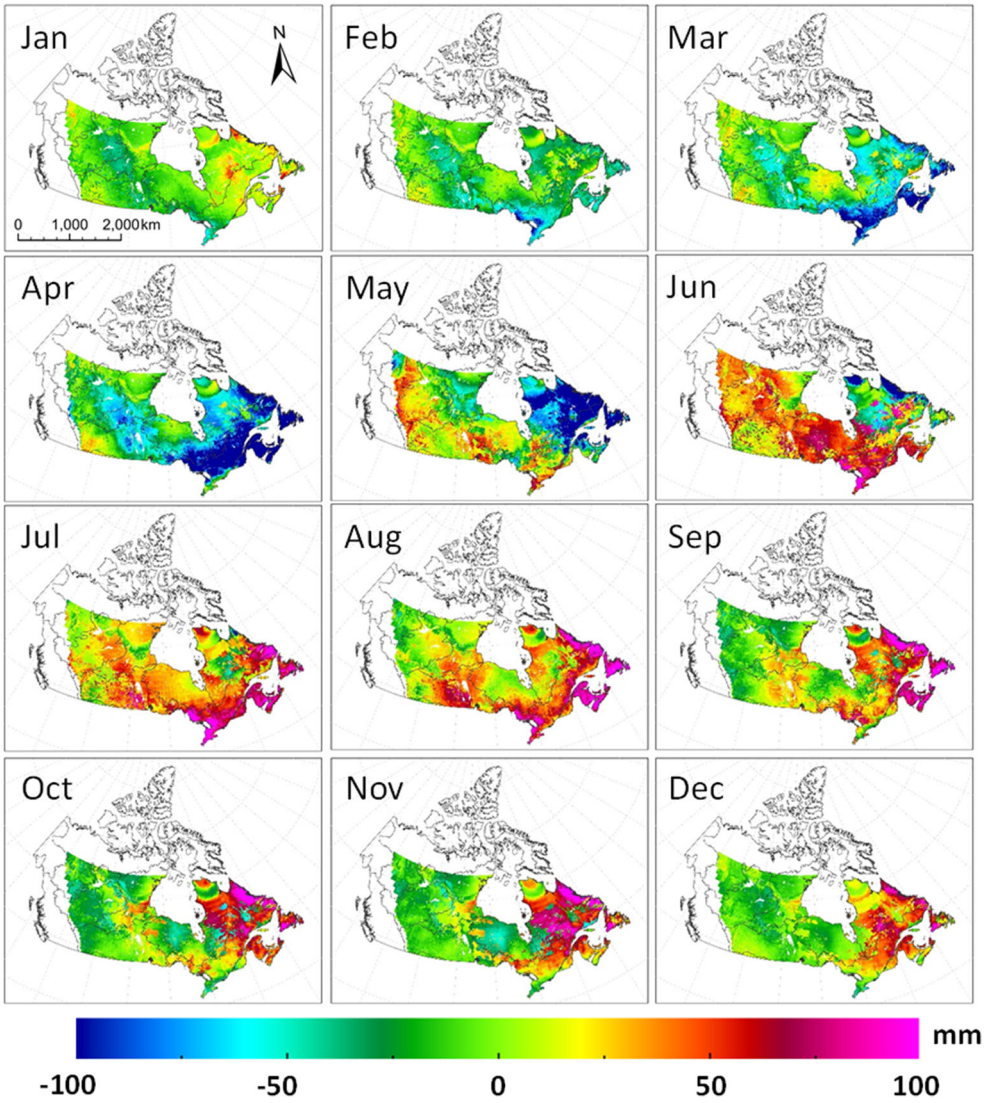

Fig. 2 The average monthly W_{ground} over 2003–2016, showing its spatial and seasonal variations over the landmass

and reaches a high value around 75 mm above the annual average in June. The long winter in the north delays the snowmelt. As a result, the north part of east Canada has 1–2 months delay to reach the lowest W_{ground}—for example, the north portion of the St. Lawrence MDA and the Northern Quebec and Labrador MDA reach the lowest W_{ground} (~75 mm below the annual average) mostly 1 month later in May and the north Labrador portion has the lowest W_{ground} (over 100 mm below the annual average) 2 months later in June. In June, a large portion of the study area shows a high W_{ground} except that the Northern Quebec and Labrador MDA still presents a low W_{ground} with the value of around 50 mm below the annual average.

In summer, the western region and the southwestern Hudson Bay area have high evapotranspiration. As a result, they lead to relatively low groundwater recharge, resulting in net water loss in these regions. Most of these regions experience rapidly decreasing W_{ground} in summer, after which the W_{ground} reaches its lowest value before winter (Fig. 2)—for example, the Arctic MDA arrives at the lowest W_{ground} (~30 mm below the annual average) mostly in October/November, while southwestern Hudson Bay indicates that it took 1 month later to reach the lowest W_{ground} (~60 mm below the annual average). In contrast, the Northern Quebec and Labrador MDA in east Canada mainly shows a rapid increase of W_{ground} in summer. These regions have high precipitation in fall, resulting in another high groundwater recharge before winter. As a result, the W_{ground} in most of these regions reaches the annual peak (e.g., over 100 mm above the annual average in north Labrador) in October or November, after which the W_{ground} rapidly decreases in January. Like in the winter and spring, south Canada also presents different seasonal patterns in W_{ground} variations during summer and fall, whereby it has substantial precipitation after spring, resulting in rapid groundwater recharge. The highest W_{ground} (e.g., over 100 mm above the annual average in the southern Ontario)

occurs in July or August, after which the W_{ground} rapidly drops in October and then gradually decrease throughout fall.

It is observed from Fig. 2 that the study area overall presents low W_{ground} in early spring and high W_{ground} in early summer. The months having the lowest/highest W_{ground} vary by regions. Figure 3a,b shows the spatial distribution of the months having maximum/minimum W_{ground} (M_{max}/ M_{min}), for 1 year for the study period. As discussed earlier, the M_{max}/ M_{min} presents large spatial differences over the study area. Generally, the study region shows M_{max} mainly in late spring and early summer, except for the Northern Quebec and Labrador MDA which has M_{max} mainly in October or November. In contrast to M_{max}, the M_{min} generally appears in early spring (April or May) for the study region, except for south Ontario and the south part of the Nelson River MDA, which have M_{min} in March and the north portion of the Southwestern Hudson Bay MDA, which has M_{min} in fall (October or November).

Figure 3c,d shows the interannual variations (σ_{max} and σ_{min}) of M_{max} and M_{min}, respectively, among the 14 years. Generally, the σ_{max} and σ_{min} both have values less than 2 months for most of the study area. As shown in Fig. 3c, the σ_{max} shows small spatial variations without pronounced patterns. In east Canada, the southern Ontario and the southern part of the Northern Quebec and Labrador MDA have σ_{max} of less than 1 month, whereas the remaining areas (e.g. far-north Quebec and the corridor along the St. Lawrence River) have σ_{max} of ~2 months. For the western region, the σ_{max} is generally larger than the east region. The σ_{min} presents small values of mainly less than 1 month in east Canada and relatively large values of up to 3 months in the western region. In east Canada, the σ_{min} presents very small spatial variations with abnormal

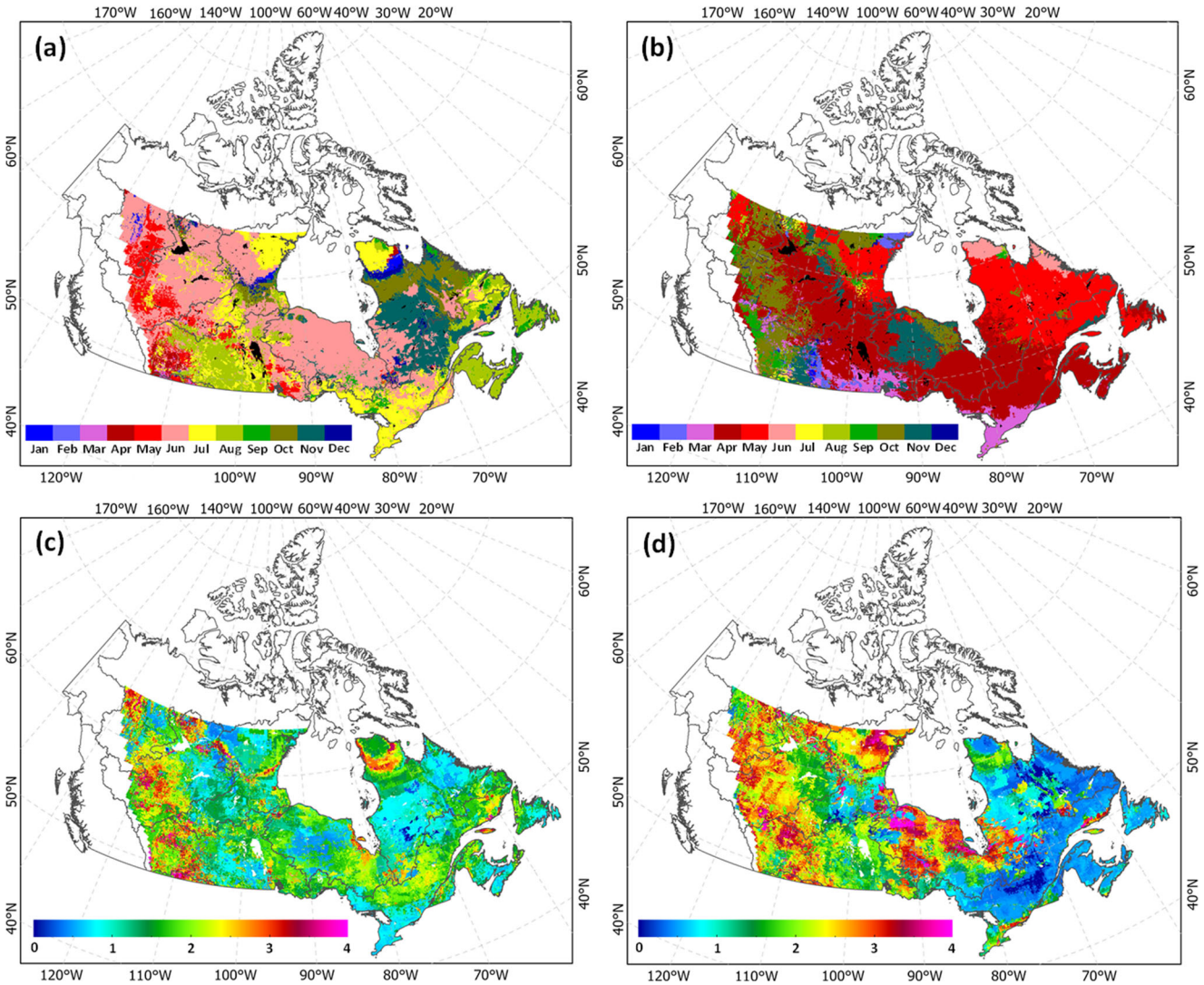

Fig. 3 The months with (**a**) maximum W_{ground} (M_{max}) and (**b**) minimum W_{ground} (M_{min}), and their interannual variations (**c**–**d**) represented by the standard deviations of M_{max} and M_{min}, respectively

values larger than 2 months in two small areas: southern Ontario and far north Quebec. For the western region, the σ_{min} in the western part is generally 1 month larger than the eastern part.

Figure 4a shows the maximum range of seasonal W_{ground} variation (ΔW_{ground}), averaged over the study period. The ΔW_{ground} presents large spatial differences with continuous increase from west to east in the study region. The large portion in east Canada has ΔW_{ground} above 250 mm, with some areas (e.g. Newfoundland island) having values of up to 400 mm. The large portion of the central area has ΔW_{ground} around 120 mm. For the western region, the ΔW_{ground} is low with the smallest ΔW_{ground} of <30 mm in the Prairie region.

The interannual variation of ΔW_{ground} among the 14 years represented by the standard deviation ($\sigma_{\Delta W ground}$), as shown in Fig. 4b, presents a similar spatial pattern to ΔW_{ground} (Fig. 4a). However, in relative terms, the interannual variations of ΔW_{ground} represented by the coefficient of variance (COV) shows small spatial differences and the COV is mostly less than 30% except in some small areas scattered over the study region such as Maritime Provinces MDA which has high values of 35–50%.

Long-term trends of W_{ground}

Figure 5 shows the trends of W_{ground} over the 14-year study period. In general, the trends present large spatial variability across the study region, mainly varying from increasing trends (i.e., water gain) of >10 mm/year to decreasing trends (i.e., water loss) of < −15 mm/year. Significant increasing trends are mainly found in east Canada (except for far north Quebec) and a central zone in northeastern Manitoba. The increasing

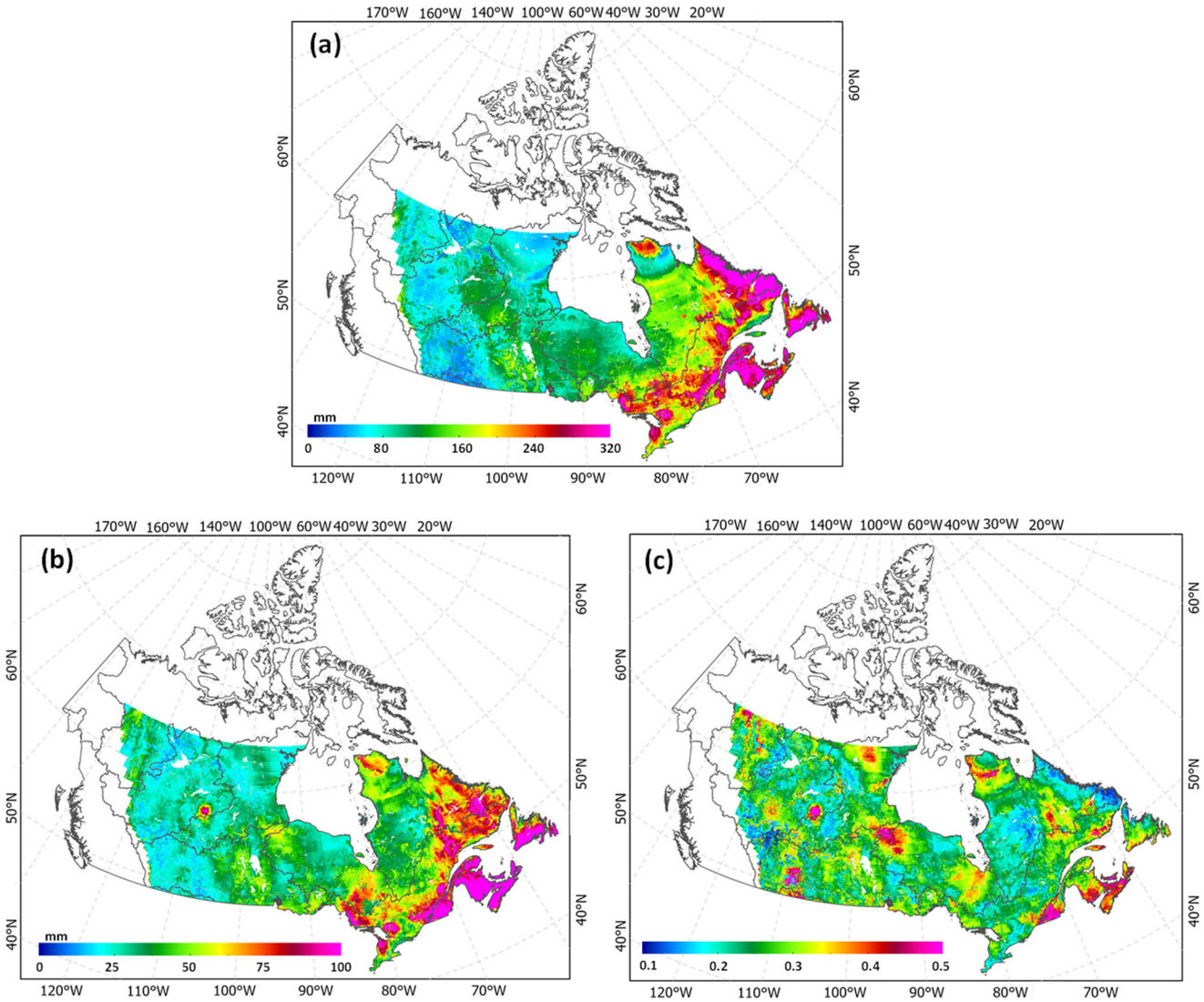

Fig. 4 (**a**) Range of seasonal variation (ΔW_{ground}) of W_{ground}, (**b**) its interannual variation represented by the standard deviation ($\sigma_{\Delta W ground}$), and (**c**) the coefficient of variance (COV)

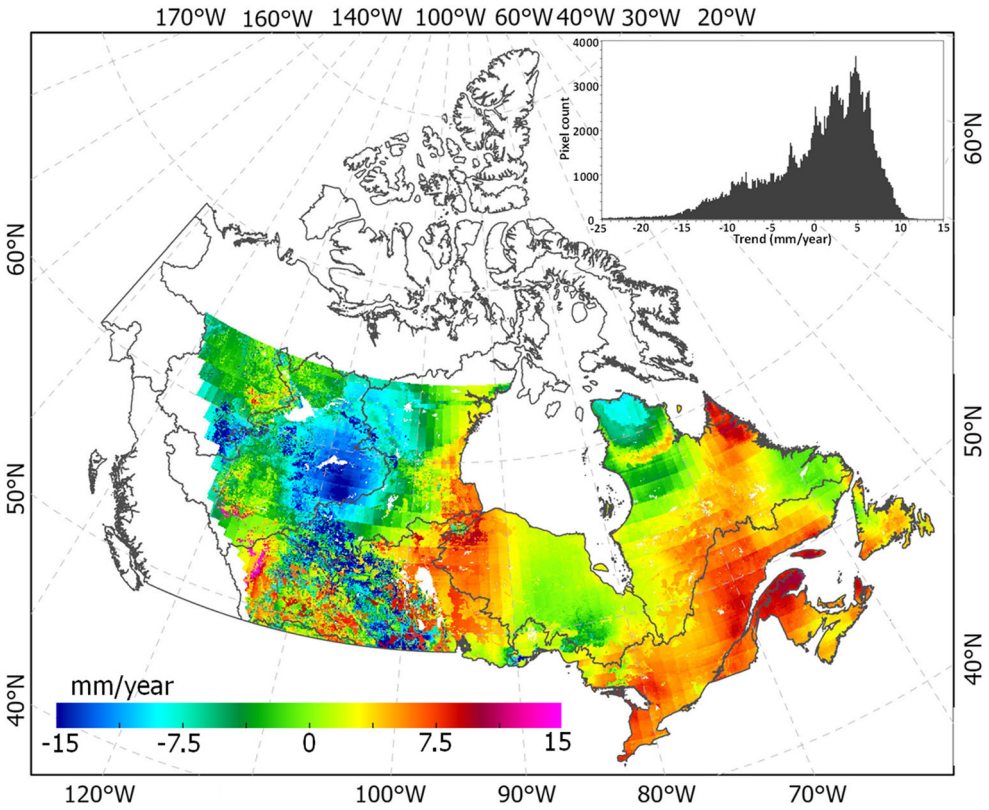

Fig. 5 The trends (mm/year) of W_{ground} over the period 2003–2016

trends of W_{ground} in east Canada are likely associated with the increase of precipitation during the study period (Li et al. 2016). The St. Lawrence MDA experienced severe drought in 2001 and 2002 and the St. Lawrence River water level plunged to its lowest point in more than 30 years, which led to a very low W_{ground} at the beginning of this study period (Wikipedia 2021). The consistent water gain over the 14 years is also a result of the recovery of W_{ground} after the severe drought. Significant decreasing trends are observed mainly in the western region. The highest decreasing trend of W_{ground} appears in some areas of the Great Slave Lake MDA. The large decreasing trends of W_{ground} in the western regions are likely due to the decrease of precipitation (Li et al. 2016).

W_{ground} for major drainage areas (MDAs)

The variations of W_{ground} for the MDAs are summarized in Table 2 and Fig. 6. The M_{max} for the Arctic and the Southwestern Hudson Bay MDAs, the Western and Northern Hudson Bay and the Great Slave Lake MDAs occurs in June, followed by the St. Lawrence MDA in July. The Maritime Provinces and the Nelson River MDAs have M_{max} in August. The Northern Quebec and Labrador MDA demonstrates late M_{max} in October. Most of the MDAs have M_{min} in April except the Northern Quebec and Labrador MDA and the Arctic MDA, having M_{min} in May and October, respectfully.

The ΔW_{ground} varied between 54.8 and 280.5 mm among the MDAs, with the highest and lowest ΔW_{ground} in the Maritime Provinces MDA and the Western and Northern Hudson Bay MDA, respectively. The three MDAs in east Canada and the Southwestern Hudson Bay MDA demonstrate ΔW_{ground} larger than 100 mm. All the four MDAs in the western region have small ΔW_{ground} values around 50–60 mm, which are less than quarter of that for the Maritime Provinces MDA. For the entire landmass, the W_{ground} reaches the high peak in July and the low peak in April (Table 2), with a ΔW_{ground} of 117.7 mm or 699.9 km^3. It is worth noting that there is large spatial variability of W_{ground} in each MDA especially in the Maritime Provinces MDA (Figs. 2 and 6).

The long-term trends of W_{ground} for the MDAs (Table 2) show that the 4 MDAs in east Canada (Maritime Provinces, St. Lawrence, Northern Quebec and Labrador, and Southwestern Hudson Bay) have increasing trends from 2003 to 2016. The Maritime Provinces MDA has the highest W_{ground} increase of 6.25 mm/year, followed by the St. Lawrence MDA having an increasing trend of 4.97 mm/year. The Northern Quebec and Labrador and the Southwestern Hudson Bay MDAs shows 1.80 and 2.45 mm/year of W_{ground} increase, respectively. Among four MDAs in the western regions, the Great Slave Lake MDA has the largest W_{ground} decrease of 6.67 mm/year. The Western and Northern Hudson Bay MDA and the Arctic MDA show W_{ground}

Table 2 The characteristics of groundwater storage (W_{ground}) for major drainage areas (MDAs)

MDA name	Area	Month with maximum W_{ground} (M_{max})	Month with minimum W_{ground} (M_{min})	Range of seasonal variations (ΔW_{ground})		Trend (τ)	
	km^2	–	–	mm	km^3	mm/year	km^3/year
Maritime Provinces	163,990	Aug	Apr	280.5	46.0	6.25	1.02
St. Lawrence	1,067,879	Jul	Apr	183.3	195.7	4.97	5.31
Northern Quebec and Labrador	1,158,292	Oct	May	135.0	156.4	1.80	2.08
Southwestern Hudson Bay	735,320	Jun	Apr	103.0	75.7	2.45	1.80
Nelson River	987,015	Aug	Apr	62.7	61.9	−0.04	−0.04
Western and Northern Hudson Bay	724,700	Jun	Apr	54.8	39.7	−3.93	−2.84
Great Slave Lake	775,150	Jun	Apr	66.8	51.8	−6.67	−5.17
Arctic	334,225	Jun	Oct	55.5	18.5	−4.76	−1.64
All MDAs	5,946,572	Jul	Apr	117.7	699.9	0.002	0.01

decrease of 3.93 and 4.76 mm/year, separately. For the Nelson River MDA, although the entire drainage area has a slight decreasing trend of −0.04 mm/year, it presents large spatial variability with increasing trends of up to 8 mm/year in some areas of western portion (mainly in Prairie pothole region) and decreasing trends of up to −15 mm/year in some areas of the eastern portion. For the entire study region, a slight increase of 0.002 or 0.01 km^3/year of overall W_{ground} demonstrates that there is no significant trend over the 14-year period of 2003–2016.

Comparisons of different GRACE solutions

The W_{ground} discussed in the preceding analyses is based on the GRACE SH solutions. The results are compared with those derived from two GRACE Mascon solutions—JPL Mascon solution (JPL-MSCN) and CSR Mascon solution (CSR-MSCN)—in Fig. 7 and Table 3. Generally, the W_{ground} derived from all three solutions presents highly consistent seasonal patterns and trends for all the MDAs, although the Maritime Provinces MDA and the Arctic MDA present relatively large differences among the three solutions. More specific comparisons, which include correlation coefficients (R) and root mean square errors (RMSE), are summarized in Table 3. The SH W_{ground} is highly correlated to those derived from JPL Mascon solution (R range 0.75–0.97) and CSR Mascon solution (R range 0.83–0.98). The largest differences between SH and the two Mascon solutions occur in the Maritime Provinces, with RMSE of 49.4 mm for SH vs. JPL-MSCN and 28.9 mm for SH vs. CSR-MSCN, followed by the Arctic MDA having RMSE of 22.4 and 18.9 mm for the JPL-MSCN and the CSR-MSCN, respectively. The smallest differences between SH and the Mascon solutions occur in the Northern Quebec and Labrador and the Western and Northern Hudson Bay MDAs (Table 3). For the entire study region, the SH-derived W_{ground} has a R value of 0.94 with JPL-MSCN and 0.98 with CSR-MSCN. The corresponding RMSEs are 10.5 and 5.58 mm, respectively.

Comparisons to groundwater level (W_{level}) measurements

Due to the difficulty in acquiring groundwater storage observations, this study compares the SH-derived W_{ground} to the groundwater level (W_{level}) measured in wells in this study area. Observations from a total of 10 wells, with 4 wells within a GRACE SH grid in the Nelson River MDA and 6 wells within a GRACE SH grid in the St. Lawrence MDA, are used (Fig. 1). The relationships (R values) between each two W_{level} measurements vary from 0.047 to 0.821 with a mean value of 0.46 for the grid in the Nelson River MDA, and from 0.3 to 0.94 with a mean value of 0.56 for the grid in the St. Lawrence MDA. The low correlations among the wells in each grid are partially due to the relatively large measurement uncertainties compared with the small W_{level} variations. Figure 8 compares the time series of GRACE-based W_{ground} and W_{level} (well average) over the study period for the two GRACE SH grids. The W_{ground} and W_{level} present similar trends in both grids. For the grid in the Nelson River MDA (Fig. 8a), both W_{ground} and W_{level} show four subtrends during the study period, i.e., increasing trends for the period 2003–2006, decreasing trends during the period 2006 to 2009, increasing trends from 2009 to 2011, and decreasing trends in 2011–2016. For the grid in the St. Lawrence MDA (Fig. 8b), both W_{ground} and W_{level} do not present notable long-term trends. The correlation coefficients between W_{ground} and W_{level} are 0.3 for the Nelson River MDA, and 0.26 for the St. Lawrence MDA. It is observed that the W_{ground} and W_{level} seasonal variations show phase differences, which partially result in the low correlation coefficients between W_{ground} and W_{level}. The phase differences can be

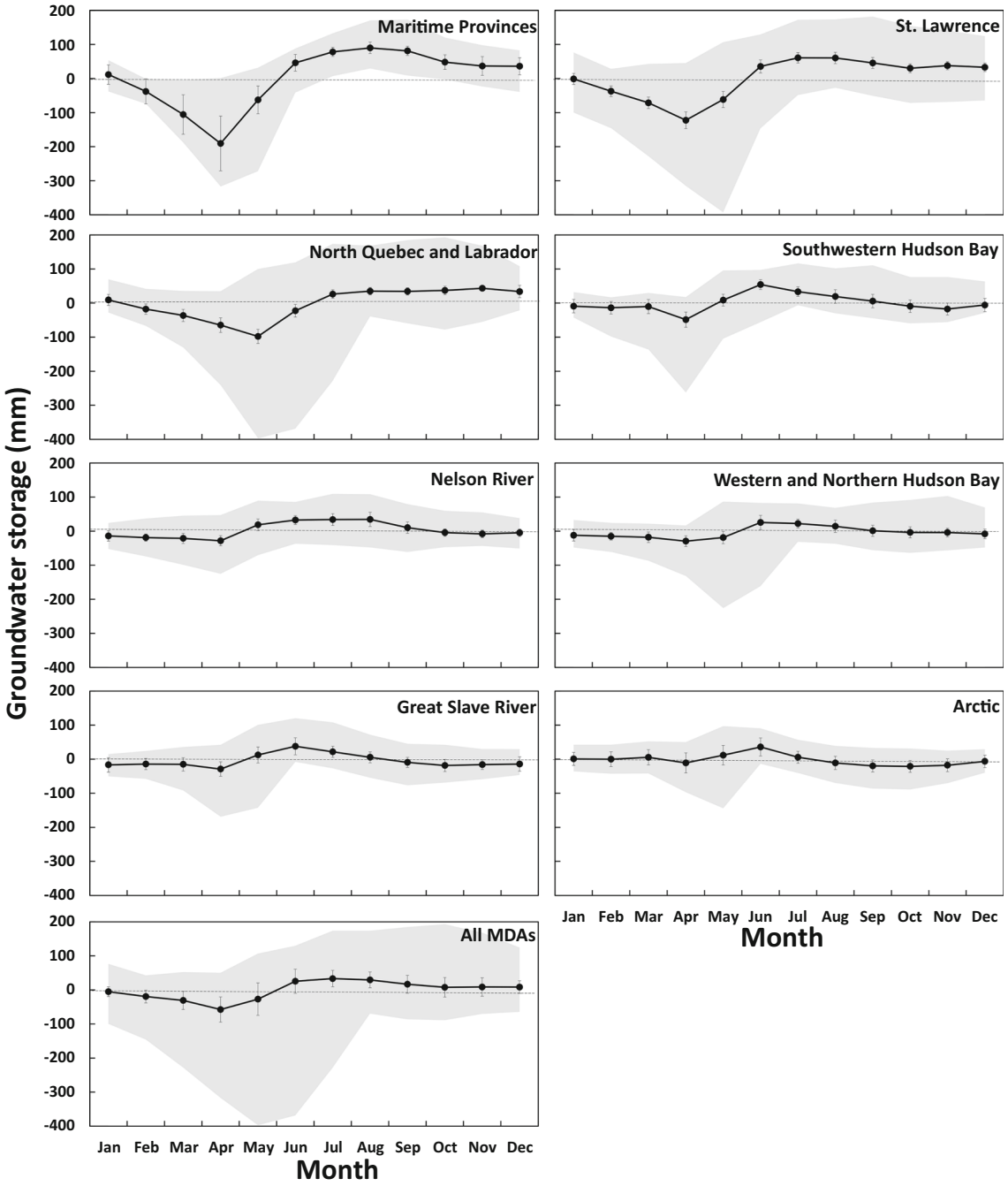

Fig. 6 Seasonal variations of W_{ground} for the MDAs in the study area. The black lines represent the average monthly W_{ground} over 2003–2016. The grey areas represent the W_{ground} variation ranges in 2003–2016. The error bars show the spatial variability of the W_{ground} in the MDAs, represented by its standard deviations

clearly seen from the monthly average values shown in Fig. 9. Generally, the W_{ground} shows the seasonal pattern 1 month earlier than the W_{level} for the grid in Nelson River MDA. When moving the W_{level} data 1 month forward, the R increases to 0.37 from 0.3. For the grid in the St. Lawrence MDA, the W_{ground} and W_{level} show different phase differences. After moving the W_{ground} time series 1 month forward, the R between W_{ground} and W_{level} increases to 0.51 from 0.26.

The range of seasonal variation for W_{level} and W_{ground} is ~0.2 m (ΔW_{level}) and ~40 mm (ΔW_{ground}), respectively, for the grid in the Nelson River MDA. The grid in the St. Lawrence MDA has ΔW_{level} of ~1.0 m and ΔW_{ground} of ~110 mm. Both grids show large variabilities of W_{level} among the well measurements (standard deviation of ~0.4 m for the grid in the Nelson River MDA and ~0.6 m for the grids in the St. Lawrence MDA, see Fig. 9). The large differences can also

Table 3 Comparisons of W_{ground} derived from the spherical harmonic solution, the JPL Mascon solution, and the CSR Mascon solution

MDA name	JPL Mascon solution		CSR Mascon solution	
	R	RMSE (mm)	*R*	RMSE (mm)
Maritime Provinces	0.89	49.4	0.96	28.9
St. Lawrence	0.97	14.7	0.98	12.1
Northern Quebec and Labrador	0.97	10.9	0.98	9.9
Southwestern Hudson Bay	0.94	12.7	0.95	10.8
Nelson River	0.87	17.5	0.91	12.6
Western and Northern Hudson Bay	0.88	13.9	0.95	8.84
Great Slave Lake	0.94	13.5	0.96	10.4
Arctic	0.75	22.4	0.83	18.9
All MDAs	0.95	10.5	0.98	5.58

R correlation coefficient; *RMSE* root mean square error

be seen from the low correlation coefficients among the well measurements as discussed in the preceding. It is noted that the variability of W_{level} among the well measurements is twice that of the seasonal variation range (ΔW_{level}) for the grid in the Nelson River MDA, and about half of the ΔW_{level} for the grid in the St. Lawrence MDA, suggesting relatively large uncertainty in W_{level} measurements and small variations of the W_{level} signal. This poses large challenges for directly comparing GRACE-based groundwater estimations with in-situ well measurements, and it is a major reason for the low *R* values between W_{ground} and W_{level} discussed in the preceding.

Discussion

In this study, W_{ground} is estimated using the GRACE-observed TWS and LSM-based W_{soil}, W_{snow}, and W_{surf} from the EALCO model. Errors or uncertainties in TWS, W_{soil}, W_{snow}, and W_{surf} estimates would directly propagate to W_{ground}. Mortimer et al. (2020) evaluated nine Northern Hemishphere gridded W_{snow} products from three categories—reanalysis models, passive microwave remote sensing combined with surface observations, and standalone passive microwave retrievals. Evaluation against snow course measurements in Canada shows high RMSE and bias, and low correlation. The uncertainty for all products tends to increase with deeper snow. Results showed the errors (RMSE as a percentage of mean in-situ W_{snow}) are larger than 50% for Canada. Xia et al. (2015) used soil-moisture observations from seven observational networks in USA with different biome and climate conditions to evaluate soil-moisture products simulated from four LSMs, including Noah, Mosaic, SAC (Sacramento soil moisture accounting), and VIC (Variable Infiltration Capacity model). The errors (RMSE as a percentage of mean in-situ soil moisture) show that strong seasonal variations varied by model and soil layer, having values larger than 20% for most of the observational networks. The EALCO model used in this study is developed in Canada with comprehensive algorithms for cold-region processes, and has undergone extensive calibration and validation for the Canadian landmass (e.g., Zhang et al. 2008; Widlowski et al. 2011; Wang et al. 2014, 2015a, b); therefore, the errors in the estimates for these water variables are expected to be smaller in this study than those discussed in the preceding.

GRACE-observed TWS errors, including errors from measurements, spatial and spectral leakages, post-processing, and GIA adjustment, would also bring uncertainties to the W_{ground} estimates. The combined error from measurements and leakages depends on the drainage area/basin size (Zhang et al. 2016; Wang et al. 2014; Landerer and Swenson 2012). Generally, it would be within 15 mm at the MDA level in Canada. It is worth noting that the GIA uplift rates are mostly under 10 mm/year in Canada (Fatolazadeh and Goita 2021; Argus et al. 2021), which is much smaller than the magnitudes of seasonal variations of the TWS signal. Thus, the GIA impact on the water characterization is more likely on the long-term trend rather than the seasonal patterns.

Integrating all the errors from TWS, W_{soil}, W_{snow} and W_{surf}, Frappart and Ramillien (2018) showed that the errors on trend estimates of W_{ground} derived from GRACE observations and LSMs were around 10% or less in several areas/basins around the world (e.g., 9.5% in the California Central Valley (USA), Scanlon et al. 2012; 13.6% in the north of China, Feng et al. 2013; 7.14% in Colorado Basin (USA), Castle et al. 2014; and 2.2% in the Tigris and the Euphrates Basin (Asia), Voss et al. 2013). In cold regions like Canada, snow and ice are important features of the landscape. W_{snow} is a primary contribution to TWS in winter time. The large uncertainty of LSM-based estimates of W_{snow} might significantly impact accuracy of the GRACE-derived W_{ground}. Directly quantifying the uncertainty of W_{ground} is still difficult due to the lack of independent data and it needs to be addressed in future studies.

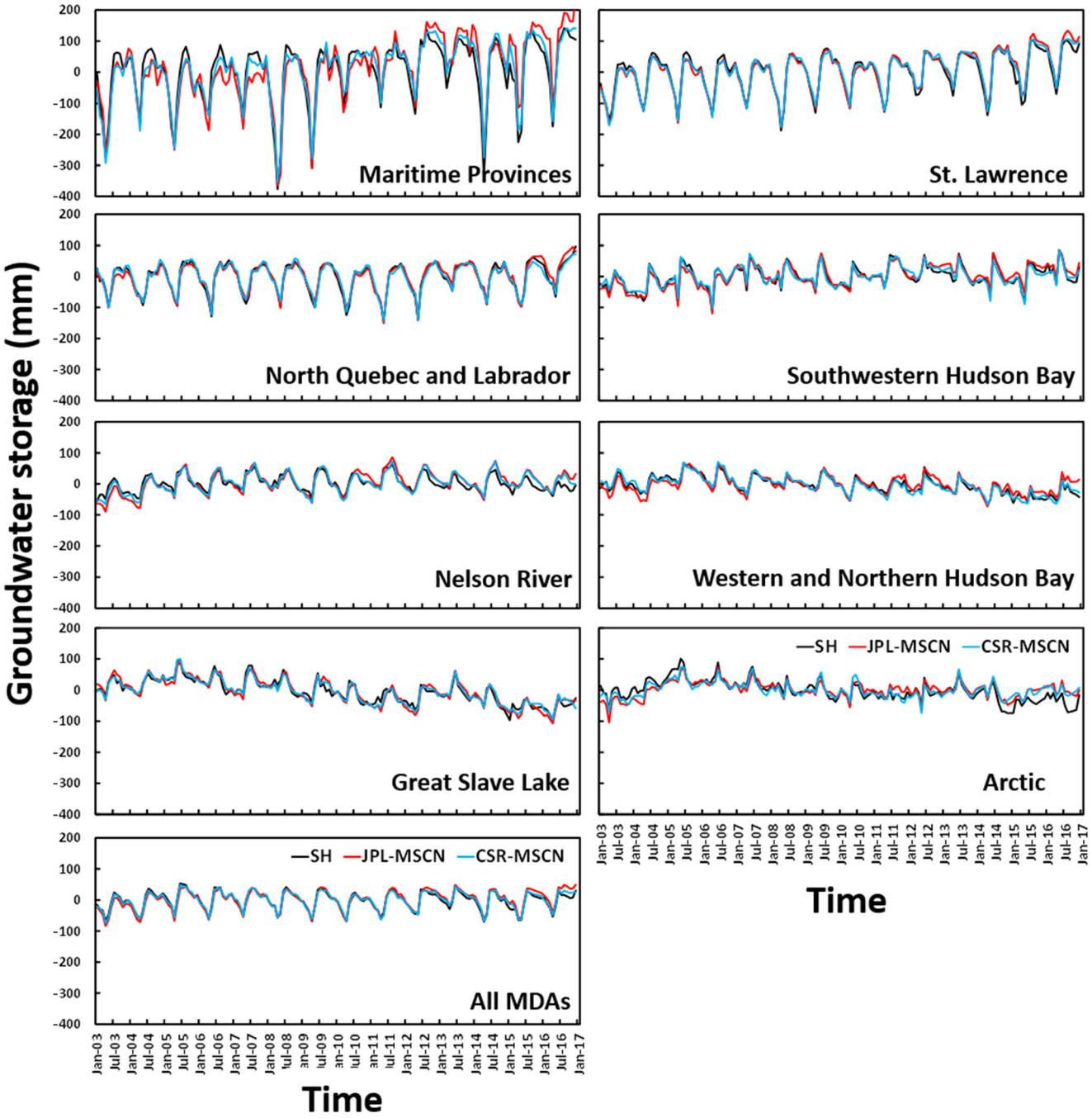

Fig. 7 Time series of monthly W_{ground} derived from three GRACE solutions over the period 2003–2016: the GRACE spherical harmonic solution (SH), the Jet Propulsion Laboratory Mascon solution (JPL-MSCN) and the Center for Space Research Mascon solution (CSR-MSCN)

Summary

Using the GRACE-based TWS and the EALCO modelled W_{soil}, W_{snow}, and W_{surf}, the seasonal variations and trends of the W_{ground} over a large portion of Canada's landmass for the period of 2003–2016 were assessed. It is observed that the overall W_{ground} has maximum/minimum values in July/April with a seasonal variation range (ΔW_{ground}) of 118 mm (or 700 km^3) for the landmass. East Canada has relatively large ΔW_{ground} mainly in the range of 200–250 mm with the largest values of up to 400 mm in the Newfoundland. The west region has relatively small ΔW_{ground}, mostly around 125 mm, with the smallest values (lower than 50 mm) appearing in the Prairie area. The months having the maximum and the minimum groundwater storage (M_{max} and M_{min}) vary by regions. The western region and the Southwestern Hudson Bay major

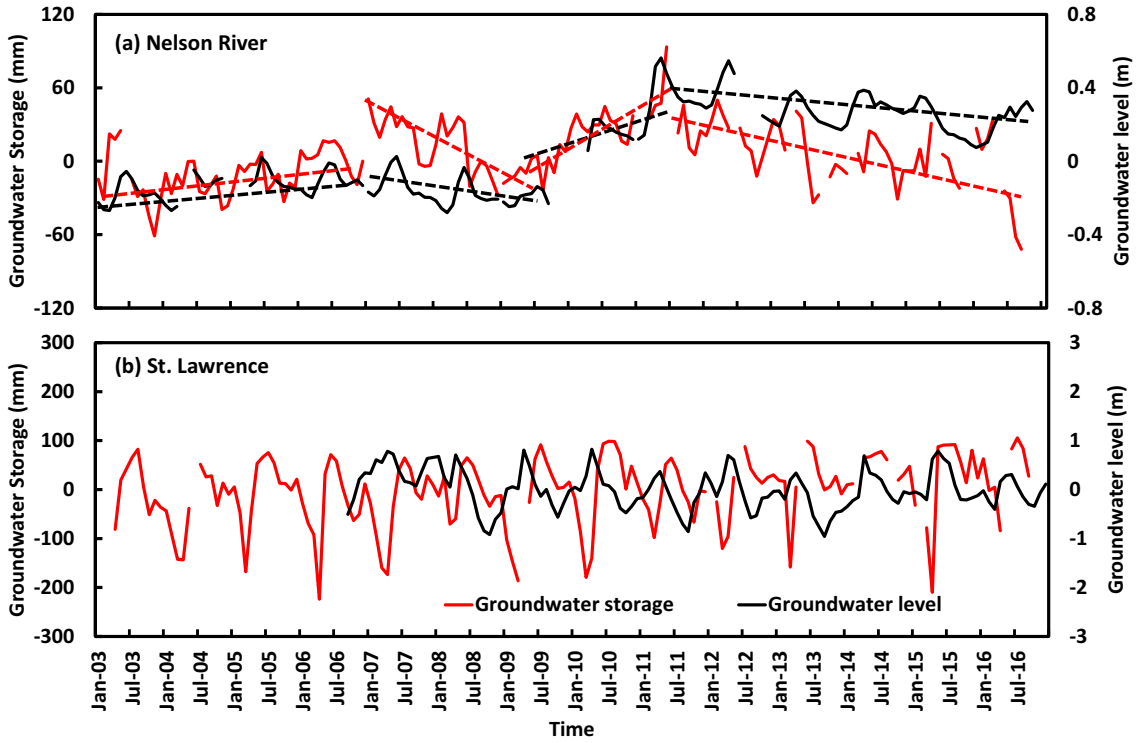

Fig. 8 Variations of W_{ground} and W_{level} for grids in **a** the Nelson River MDA and **b** the St. Lawrence MDA over the period 2003–2016

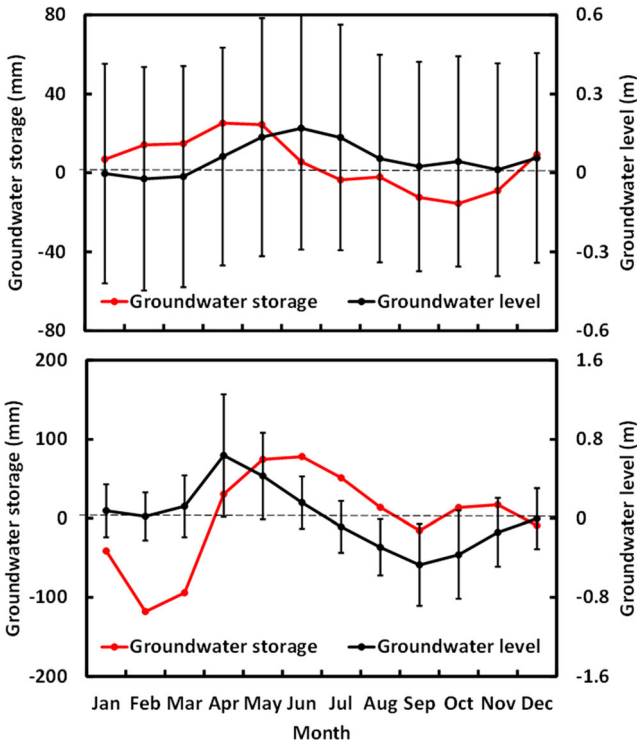

Fig. 9 Average monthly W_{ground} and W_{level} over the study period for grids in **a** the Nelson River MDA and **b** the St. Lawrence MDA. The vertical bars show variability of W_{level} among the observation wells, represented by the standard deviations

drainage area (MDA) have the M_{max} and M_{min} mainly in spring and fall, respectively, while, in contrast, east Canada has the M_{max} and M_{min} mostly in fall and spring, respectively. The trend analyses over the study period indicate that significant increasing trends or water gains of up to 10 mm/year are observed in east Canada (except for far north Quebec). Significant decreasing trends or water loss are mainly observed in the central-west region with values of above −10 mm/year. The increasing trend largely offsets the decreasing trend in the study area, and the overall W_{ground} for the entire landmass does not show a significant trend over 2003–2016. The comparison of W_{ground} from the GRACE spherical harmonic solution and two Mascon solutions shows that they present consistent seasonal patterns and trends. The comparison of GRACE-based W_{ground} with groundwater well measurements shows that they present similar long-term trends but with phase difference (~1 month) in seasonal variations.

Supplementary Information The online version contains supplementary material available at https://doi.org/10.1007/s10040-022-02460-1.

Funding This study is supported by the Cumulative Effects Project of the Natural Resources Canada.

Declarations

Conflict of interest There is no conflict of interest for this paper.

References

Argus DF, Peltier WR, Blewitt G, Kreemer C (2021) The viscosity of the top third of the lower mantle estimated using GPS, GRACE, and relative sea level measurements of glacial isostatic adjustment. J Geophys Res: Solid Earth 126:e2020JB021537. https://doi.org/10.1029/2020JB021537

Bahanja SN, Zhang X, Wang J (2018) Estimating long-term groundwater storage and its controlling factors in Alberta, Canada. Hydrol Earth Syst Sci 22:6241–6255. https://doi.org/10.5194/hess-22-6241-2018

Castle Sl, Thomas BF, Reager JT, Rodell M, Swenson SC, Famiglietti JS (2014) Groundwater depletion during drought threatens future water security of the Colorado River basin. Geophys Res Lett 41:5904–5911

Chen J, Li J, Zhang Z, Ni S (2014) Long-term groundwater variations in Northwest India from satellite gravity measurements. Glob Planet Chang 116:130–138. https://doi.org/10.1016/j.gloplacha.2014.02.007

Chen J, Famiglietti JS, Scanlon BR, Rodell M (2016) Groundwater storage changes: present status from GRACE observations. Surv Geophys 37(2):397–417. https://doi.org/10.1007/d10712-015-9332-4

Council of Canadian Academies (2009) The sustainable management of groundwater in Canada, Report of the expert panel on groundwater. Council of Canadian Academies, Ottawa, Canada

Famiglietti JS, Lo M, Ho SL, Bethune J, Anderson KJ, Syed TH, Swenson SC, de Linage CR, Rodell M (2011) Satellites measure recent rates of groundwater depletion in California's Central Valley. Geophys Res Lett 38:L03403. https://doi.org/10.1029/2010GL046442

Fatolazadeh F, Goita (2021) Mapping terrestrial water storage changes in Canada using GRACE and GRACE-FO. Sci Total Environ 779(2):146435. https://doi.org/10.1016/j.scitotenv.146435

Feng W, Zhong M, Lemoine J-M, Biancale R, Hsu H-T, Xia J (2013) Evaluation of groundwater depletion in North China using the gravity recovery and climate experiment (GRACE) data and ground-based measurements. Water Resour Res 49:2110–2118

Frappart F, Ramillien G (2018) Monitoring groundwater storage changes using the gravity recovery and climate experiment (GRACE) satellite mission: a review. Remote Sens 10(6):829. https://doi.org/10.3390/rs10060829

GIN (2021) Groundwater Information Network, http://gw-info.net. Accessed 1 July 2021

Huang J, Pavlic G, Rivera A, Palombi D, Smerdon B (2016) Mapping groundwater storage variations with GRACE: a case study in Alberta, Canada. Hydrol J 24:1663–1680. https://doi.org/10.1007/s10040-016-1412-0

JLP (2020) Gravity Recovery and Climate Experiment (GRACE). NASA Jet Propulsion Laboratory. https://podaac.jpl.nasa.gov/GRACE. Accessed 1 June 2020

Landerer F (2020) CSR TELLUS GRACE Level-3 monthly land water-equivalent thickness surface mass anomaly Release 6.0 version 03 in netCDF/ASCII/GeoTiff format. Ver. RL06 v03. PO.DAAC, CA, USA. https://podaac.jpl.nasa.gov/dataset/TELLUS_GRAC_L3_CSR_RL06_LND_v03. Accessed January 2022

Landerer F, Swenson SC (2012) Accuracy of scaled GRACE terrestrial water estimates. Water Resour Res 48:W04531. https://doi.org/10.1029/2011WR011453

Li J, Wang S, Zhou F (2016) Time series analysis of long-term terrestrial water storage over Canada from GRACE satellites using principal component analysis. Can J Remote Sens 42(3):161–170. https://doi.org/10.1080/07038992.2016.1166042

Mortimer C, Mudryk L, Derksen C, Luojus K, Brown R, Kelly R, Tedesco M (2020) Evaluation of long-term Northern Hemisphere snow water equivalent products. The Cryosphere 14(5):1579–1594. https://doi.org/10.5194/tc-14-1579-2020

Opie S, Taylor RG, Brierley CM, Shamsudduha M, Cuthbert MO (2020) Climate-groundwater dynamics inferred from GRACE and the role of hydraulic memory. Earth Syst Dynam 11:775–791. https://doi.org/10.5194/esd-11-775-2020

QGMN (2021) Quebec Groundwater Monitoring Network, https://www.environnement.gouv.qc.ca/eau/piezo/index.htm. Accessed 1 July 2021

Richey AS (2014) Stress and resilience in the world's largest aquifer systems: a GRACE-based methodology. PhD Thesis, University of California, Irvine, CA

Rodell M, Chen J, Kato H, Famiglietti JS, Nigro J, Wilson CR (2007) Estimating groundwater storage changes in the Mississippi River basin (USA) using GRACE. Hydrol J 15:159–166

Rodell M, Velicogna I, Famiglietti JS (2009) Satellite-based estimates of groundwater depletion in India. Nature 460:999–1002. https://doi.org/10.1038/nature08238

Scanlon BR, Longuevergne L, Long D (2012) Ground referencing GRACE satellite estimates of groundwater storage changes in the California Central Valley, USA. Water Resour Res 48(4):W04259. https://doi.org/10.1029/2011WR011312

Shamsudduha M, Taylor RG (2020) Groundwater storage dynamics in the world's large aquifer systems from GRACE: uncertainty and role of extreme precipitation. Earth Syst Dynam 11:755–774. https://doi.org/10.5194/esd-11-755-2020

Statistics Canada (2003) Standard Drainage Area Classification (SDAC). Available at http://www.statcan.gc.ca/subjects-sujets/standard-norme/sdac-ctad/sdac-ctad-eng.htm. Accessed 2 June 2020

Swenson SP, Yeh J-F, Wahr J, Famiglietti J (2006) A comparison of terrestrial water storage variations from GRACE with in situ measurements from Illinois. Geophys Res Lett 33:L16401. https://doi.org/10.1029/2006GL026962

Tapley BD, Bettadpur S, Watkins M, Reigber C (2004) The gravity recovery and climate experiment: mission overview and early results. Geophys Res Lett 31:L09067. https://doi.org/10.1029/2004GL019920

Thomas BF, Famiglietti JS (2019) Identifying climate-induced groundwater depletion in GRACE observations. Nat Sci Rep 9:4124. https://doi.org/10.1038/s41598-019-40155-y

Trishchenko AP, Ungureanu C (2021) Minimum snow/ice extent over northern circumpolar landmass in 2000-2019: how much snow survives the summer melt? Bull Am Meteorol Soc. https://doi.org/10.1175/BAMS-D-20-0177.1

Voss KA, Famiglietti JS, Lo M, de Linage C, Rodell M, Swenson SC (2013) Groundwater depletion in the Middle East from GRACE with implications for transboundary water management in the Tigris-Euphrates-Western Iran region. Water Resour Res 49:904–914

Wang S, Li J (2016) Terrestrial water storage climatology for Canada from GRACE satellite observations in 2002–2014. Can J Remote Sens 42(3):190–202. https://doi.org/10.1080/07038992.2016.1171132

Wang S, Huang J, Li J, Rivera A, McKenney DW, Sheffield J (2014) Assessment of water budget for sixteen large drainage basins in Canada. J Hydrol 512:1–15. https://doi.org/10.1016/j.jhydrol.2014.02.058

Wang S, Pan M, Mu Q, Shi X, Mao J, Brummer C, Black TA (2015a) Comparing evapotranspiration from eddy covariance measurements, water budgets, remote sensing, and land surface models over Canada. J Hydrometerorol 16(4):1540–1560

Wang S, Huang J, Yang D, Pavlic G, Li J (2015b) Long-term water budget imbalances and error sources for cold region drainage basins. Hydrol Process 29(9):2125–2136

Widlowski J-L, Pinty B, Clerici M, Dai Y, Kauwe D, de Ridder K, Kallel A, Kobayashi H, Lavergne T, Ni-Meister W, Olchev A, Quaife T, Wang S, Yang W, Yang Y, Yuan H (2011) RAMI4PILPS: an intercomparison of formulations for the partitioning of solar radiation in land surface models. J Geophys Res 116:G02019. https://doi.org/10.1029/2010JG00151

Wiese DN, Yuan D-N, Boening C, Landerer FW, Watkins MM (2018) JPL GRACE Mascon Ocean, Ice, and Hydrology Equivalent Water Height Release 06 Coastal Resolution Improvement (CRI) Filtered Version 1.0. Ver. 1.0. PO.DAAC, CA, USA. Dataset accessed [2020-06-01] at https://doi.org/10.5067/TEMSC-3MJC6

Wikipedia (2021) Drought in Canada. https://en.wikipedia.org/wiki/Drought_in_Canada. Accessed January 31, 2021

Xia Y, Ek MB, Wu Y, Ford T, Quiring SM (2015) Comparison of NLDAS-2 simulated and NASMD observed daily soil moisture, part I: comparison and analysis. J Hydrometeorol 16:1962–1980. https://doi.org/10.1175/JHM-D-14-0096.1

Zhang Y, Wang S, Barr AG, Black TA (2008) Impact of snow cover on soil temperature and its simulation in the EALCO model. Cold Reg Sci Technol 52:355–370. https://doi.org/10.1016/j.coldregions.2007.07.001

Zhang L, Dobslaw H, Thomas M (2016) Globally gridded terrestrial water storage variations from GRACE satellite gravimetry for hydrometeorological applications. Geophys J Int 206:368–378